Keywords : medical imaging, blood vessels,
3D images, image processing,
segmentation, model

Maciej ORKISZ, Marcela HERNÁNDEZ HOYOS *

MODELS FOR 3D VASCULAR IMAGE ANALYSIS

In image processing, models are used to improve robustness of algorithms by introducing *a priori* knowledge. Deformable models, frequently used in the field of medical images, are described by means of energy functionals with data attachment terms and regularising terms. The regularising terms express constraints relating to the expected shapes. The expected shape of a blood vessel segment in 3D images obtained by Magnetic Resonance Imaging or by helicoidal Computed Tomography is often implicitly described by a generalised cylinder model, *i.e.* an association of an axis (vessel centreline) and a surface (vessel boundary). In this context, the data attachment terms involve, for candidate points, a measure of the likelihood of being located on the centreline or on the boundary. Such a measure can use models reflecting low-level local photometrical properties of the brightness patterns. This presentation will give an overview of the recently used models and will be illustrated by the authors' contribution.

5. INTRODUCTION

Three-dimensional (3D) imaging techniques, namely computed tomography angiography (CTA) and magnetic resonance angiography (MRA), meet a growing success in diagnosis, treatment planning and follow-up of vascular pathologies. These techniques provide rich anatomical information which is not directly available with standard 2D X-ray digital subtraction angiography (DSA). Moreover, MRA is not invasive for the patient. However, due to limitations of contrast agent quantity and of image acquisition time, the current 3D images are relatively noisy and small blood vessels appear poorly contrasted. Their legible visualisation as well as reproducible quantification of the vascular pathologies such as stenosis and aneurysm, require appropriate image processing techniques capable to cope with these difficulties. An improved visualisation can be obtained by an adequate filtering or image enhancement technique capable of distinguishing thin vessels from noise. However, the key operation for both visualisation (namely surface rendering) and quantification is image segmentation, *i.e.* separating the vascular structures from the surrounding tissues.

It is well-known that robustness of image segmentation techniques dealing with noisy and poorly contrasted data, can be improved when exploiting *a priori* knowledge. This prior knowledge of the characteristics of the objects to be segmented and/or of the imaging process is usually introduced by means of a model. In the field of the vascular images, several levels of models are used. The highest level describes branching structures and includes anatomical knowledge of

* CREATIS UMR CNRS #5515, INSA de Lyon, bât. Blaise Pascal, 7 rue J. Capelle, 69621 Villeurbanne cedex, France

different parts of the vascular tree. An intermediate level consists in representing simple vascular segments, without bifurcations, by means of a generalised cylinder, *i.e.* an association of an axis (vessel centreline) and a surface (vessel boundary). The axis and the boundary are often detected using appropriate deformable models. As it will be detailed in the sequel of the paper, a deformable model evolves under the action of various forces, in particular image (external) forces which attract the model towards the points likely to be located respectively on the axis or on the boundary. These forces can be calculated using models of the corresponding brightness patterns. These are the lowest-level models, also useful in the design of filters and of enhancement operators.

In the following sections, these different levels of vascular models will be detailed, starting from the lowest level. This survey will be illustrated by our own contributions with a particular focus on the intermediate-level models useful in the segmentation and quantification of diseased vascular segments.

5. LOW-LEVEL MODELS OF ORIENTED BRIGHTNESS PATTERNS

The goal of the angiography imaging techniques is to amplify the signal of the vessel lumen compared to the surrounding tissues. Consequently, in most of the angiography images, the vessels are brighter than the background. This simplest model of the grey-level distribution still holds after inverting the grey scale in the so called “black blood” angiography images. Based on this model, segmentation can be done using a threshold [9, 28, 33, 49, 60]. To make the segmentation reproducible, the choice of an appropriate threshold needs to be done automatically. Such an automatic choice of the threshold requires a finer model of the grey-level distribution. It has been shown that the actual distribution depends on the imaging modality: *e.g.* in the time-of-flight MRA images the distribution can be approximated by a combination of two Gaussians and of a uniform distribution [54], while in the phase-contrast MRA images the background noise has a Rician distribution and the circulating blood signal can be approximated by a uniform distribution (under laminar flow assumption) [8]. The automatic calculation of the threshold consists in identifying the parameters of the corresponding distribution model. However, when using a thus found global threshold, the segmented images generally contain only large vessels while small vessels disappear because their intensities are below the threshold. Moreover, some tissues or image acquisition artefacts may have intensities higher than the global threshold. It has been shown that the location of the vessel boundaries coincides with a certain percentage of the local intensity maximum (the percentage depends, once again, on the imaging modality) [23]. Therefore, vessel tracking algorithms were proposed, based on seeded region growing with local threshold calculation [24].

Nevertheless, higher intensity than the background is not the only characteristic of the vessels. Their most important feature is the directional (oriented) character of the corresponding brightness patterns. At an appropriate scale, each vessel can be considered as a line-like structure. Image intensity is relatively homogeneous along the line and strongly varies in other directions, namely in the planes perpendicular to the line. Similarly, the mean intensity is higher within (along) the line than in any other direction. This qualitative low-level geometrical model can be formalised in a number of ways. One of them consists in defining: 1) a set of discrete line segments, often called "sticks", centred on a current voxel (volume element, *i.e.* 3D image point) and having various orientations and 2) a "vesselness" criterion calculated for each stick and used to deduce a kind of "probability" that the central voxel belongs to a vessel and/or to estimate the local orientation of the vessel. Criteria based on such measures as mean intensity [6, 27], intensity variance [51], directional second derivatives of the intensity [10, 11] and on their combinations [36, 37] have been proposed. An example of such a criterion can be cited from [36]:

$$C_i = D_i - \alpha H_i \, , \tag{1}$$

where D_i is the average difference between the mean intensities of the i–th stick and of its parallel neighbours, while H_i is the average standard deviation of the i–th stick and of its neighbours, with a weighting constant α. This approach gives good results, but exhaustive exploration of all the possible orientations in 3D for each voxel is very time consuming.

Instead, the "vesselness" can be estimated from a few partial measurements used to build up an appropriate matrix. Many authors have proposed to exploit the eigenvalues and the eigenvectors of the Hessian matrix [12, 18, 26, 31, 44, 45]. Indeed, the local orientation of the vessels corresponds to the orientation of the eigenvector associated with the smallest (in absolute value) eigenvalue, since this eigenvector indicates the direction in which the intensity varies the least (smallest directional second derivative). The remaining two eigenvectors define the plane locally orthogonal to the vessel axis. The same reasoning applied to curvatures has led to use of the eigenvalues and of the eigenvectors of the Weingarten matrix [39, 40]. Formally, the points located on the centreline of an ideal vessel segment (*i.e.* with straight axis and circular sections) should conform to the following model:

$$\lambda_1 = 0, \ |\lambda_1| << |\lambda_2|, \ \lambda_2 = \lambda_3 \, , \tag{2}$$

where λ_i represent the eigenvalues of the considered matrix. In practice, neither the axis is necessarily straight, nor the sections are all circular (especially in the pathological cases, which are the most interesting from the clinical point of view) and the images are corrupted by noise. Hence, different "vesselness" measures proposed in the literature and based on the eigenvalues use approximations instead of equalities in (2). To illustrate this approach, let us cite the "vesselness" measure from [18]:

$$P = [1 - \exp(-R_A^2/2a^2)] \exp(-R_B^2/2b^2) [1 - \exp(-S^2/2c^2)], \tag{3}$$

where $R_A = |\lambda_2/\lambda_3|$ is a cross-sectional circularity measure, $R_B = |\lambda_1| / \sqrt{\lambda_2 / \lambda_3}$ is a measure of elongation, S is the Frobenius norm of the matrix, while a, b and c are weighting parameters. As in [25, 26, 31, 44, 45], the criterion is calculated across a range of scales and properly normalised at each scale so as to permit comparisons of the responses from different scales. The scale associated with the largest response gives an estimate of the local size of the vessel. This possibility of a multi-scale detection of the vessels, simultaneously with the estimation of their size, is an interesting feature of this approach. However, the higher the order of the derivatives, the more noise-sensitive is their computation. Hence, a low-pass filtering is usually performed prior to the computation of the derivatives, but usual isotropic filters cannot distinguish thin low-intensity vessels from noise.

An alternative approach consists in using the eigenvalues and the eigenvectors of the inertia matrix [22]. Computation of the components of the inertia matrix makes use of the image intensity instead of mass density and does not use derivation. Once again, the eigenvector associated with the smallest (in absolute value) eigenvalue λ_{min} indicates the local orientation of the vessel axis and the remaining eigenvectors define the orthogonal plane. For a vessel segment included in a sub-volume used for the matrix computation, the smallest eigenvalue is equal to the inertia moment associated with the vessel axis. Considering the model of an ideal vessel segment, with a perfectly suppressed background, there is a direct link between its diameter and this inertia moment:

$$r = \sqrt{2\lambda_{min} / M} \,, \tag{4}$$

where M is the total "mass" (intensity integral) within the cell. Hence, this approach also permits an estimation of the vessel size, although this estimation is approximate because the background never is perfectly suppressed (if it was, a simple threshold-based segmentation would be perfect!). Multi-scale processing seems possible, though it has not yet been reported.

To finish the overview of the low-level models, let us also note that the mathematical model of the oriented brightness patterns can take into account the spectral properties of the line-like structures [7, 29, 30].

5. MODELS OF VASCULAR SEGMENTS WITHOUT BIFURCATIONS

Algorithms based on the low-level models alone provide a map of "vesselness", *i.e.* each voxel is assigned a value which reflects likelihood of being located within a vessel. Usually such a map is easier to segment than the original image or, at least, provides reliable seeds for a subsequent region-growing segmentation of the original image. However, further processing of thus segmented images is necessary if quantitative results, such as lengths, diameters or section areas, are desired. This can be achieved when using higher-level geometrical models. Moreover, such models are very helpful in dealing with noisy, incomplete data. A widely used model of a vessel segment without bifurcations is a generalised cylinder, although many authors use it implicitly (maybe because this notion was “born” in the computer vision community and did not filter into the medical imaging community’s vocabulary). A generalised cylinder is defined by its axis and by its surface which is usually represented by a stack of cross-sectional contours [47]. This is a very convenient representation for the quantification purpose, since it naturally gives access to two sets of measurements: axial (length, curvature) and cross-sectional (diameter, perimeter, area, shape parameters).

There are mainly two classes of algorithms for the extraction of generalised cylinders from image data. This classification is determined by the model of the axis. Indeed, the axis can be defined as a line equidistant from the boundaries or as a set of points meeting some low level criteria such as (2). In the first case, the boundaries have to be entirely or partially extracted before the centreline extraction. Entire extraction of the boundaries supposes a preliminary segmentation using thresholds and/or region growing [14, 19, 49]. The centreline is then extracted by different variants of thinning [13, 38, 55]. Partial extraction relates to cross-sectional planar contours which are detected as the axis is iteratively constructed according to the following algorithm [50, 52, 53, 57]: 1) extract vessel boundary in the image plane orthogonal to the current axis orientation; 2) adjust the current orientation so that the axis passes through the current contour’s centre; 3) make a step forwards according to this new direction and go to 1).

In the second case, the axis can first be entirely extracted, then the cross-section generation and boundary detection can be performed as subsequent steps. The methods and the underlying models used to extract planar contours, described in the next sub-section, apply to both approaches.

5.1. PLANAR CONTOURS

Let us note that most of the models used for the extraction of cross-sectional contours are general-purpose models taking into account the specificity of the typical cross-sectional shape of the vessels. This can be illustrated by a very simple model: the contour can be defined as a line joining local maxima of intensity gradient norm greater than a threshold value, which is set to eliminate false detections due to noise. The specificity of the typical circular shape of the cross-sections can be used to perform an efficient search of these maxima. Indeed, the search can be carried out radially, starting from the estimated position of the axis within the cross-section [52, 53, 57]. Another way is to use polar co-ordinates, in which the vessel boundary should become a straight line. In this context, smooth continuous contours can be represented by a minimum-cost path model, where the cost takes into account the intensity gradient along the path [58, 59]. However, this approach can hardly cope with pathological vessels with non-circular cross-sectional shapes.

The most widely used approach of boundary extraction in medical images is based on deformable models [34]. A deformable model (curve, surface …) is defined by the expected shape properties, by some "mechanical" properties (flexibility, elasticity) and by forces which gradually deform it to make it coincide with the actual boundaries in the image. External forces attract the initial form towards the points likely to belong to a boundary (*e.g.* maximum of the gradient), while internal forces attract it towards the expected reference shape. The deformable models can be sub-divided into two classes: geometrically deformable models and parametrically deformable models. In the first case, the contour fitting is achieved by displacing the points of the contour [32, 41, 42], while in the second case it is achieved by adjusting parameters such as Fourier coefficients [48]. *A priori* knowledge of the expected shapes and of the image properties can be used to appropriately define both internal and external forces. An example of application-tailored, strongly anatomy-dependent choices (aorta in CTA) can be found in [20]. To ensure good convergence, the conventional deformable models need to be initialised close to the final solution. This can be achieved by a multi-scale search of the shapes similar to a circle [43]. Several solutions have been proposed to permit an initialisation with a single point (axis location within the cross-sectional plane). These include the use of a balloon force, which inflates the contour outwards until close vicinity of the boundaries, and a scaling process, which controls the balance between this force and the reaction force due to the elasticity of the model, independently of the contour size [21].

5.1. CENTRELINE

Like the cross-sectional boundaries, the centreline is expected to be continuous and smooth. Consequently, the models of the vessel axis, proposed in the literature, are similar to models described in the previous sub-section. Indeed, both minimum-cost path search [56] and deformable models [15-17] can be used. In the deformable model approach, the "vesselness" measure (3) was proposed to define the external force which attracts the model towards the axis. To initialise the model a small user interaction is required: the user has to select two or more points on the surface of the vessel of interest (surface rendering based on a threshold-based segmentation and on marching cubes technique, is available in most medical 3D image processing software packages). A geodesic path joining these points is used to initialise the model, which actually is a B-spline curve. Distance between the final centreline and the initial geodesic path gives an estimate of the vessel size. This is used to initialise a model of the vessel surface. Instead of a stack of cross-sectional contours, the authors proposed a deformable (active) surface defined by a product of two B-spline functions : one periodic (circumferential) and the other one aperiodic (longitudinal).

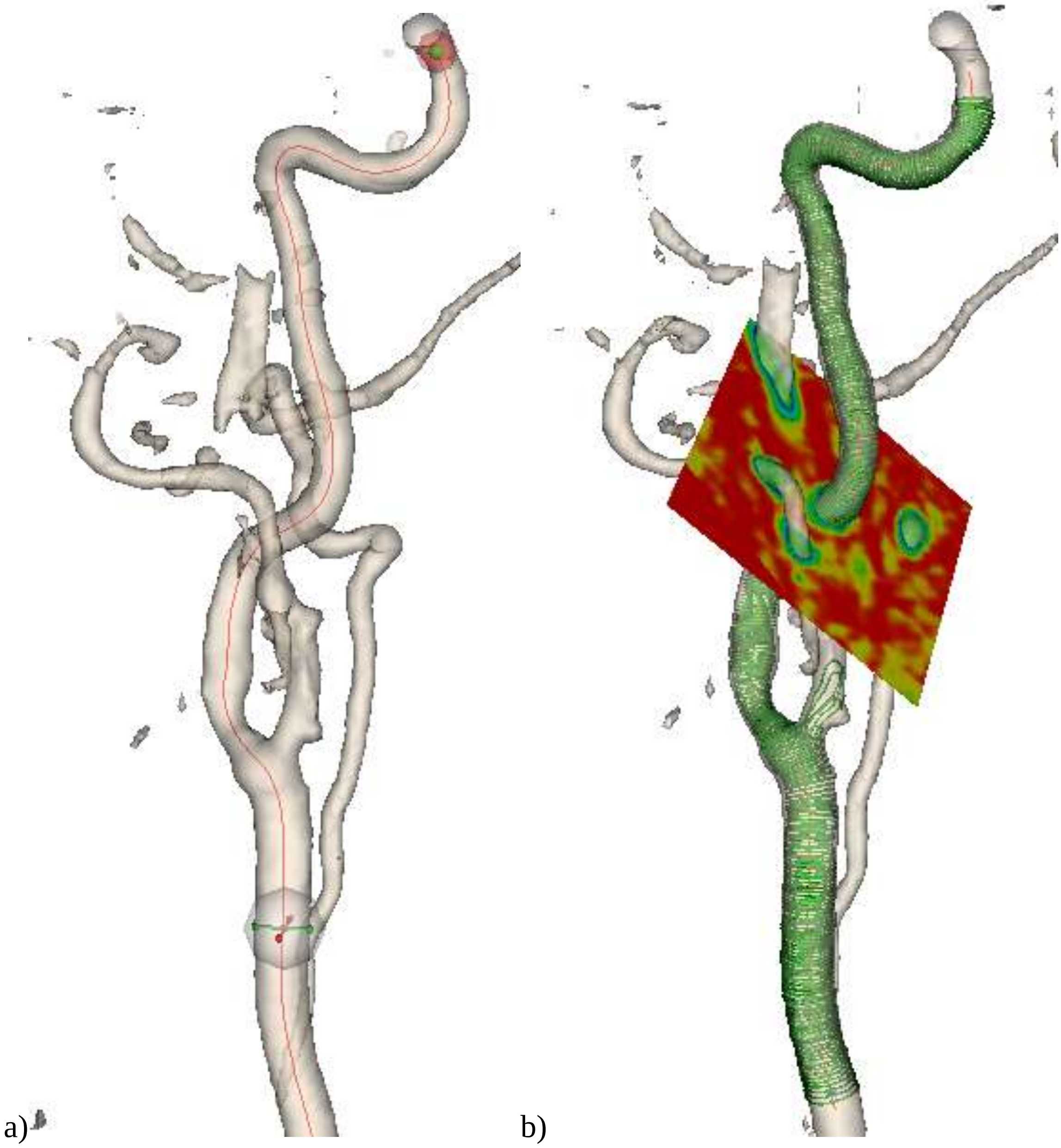

Fig 1. Vessel axis and boundary extraction for a carotid artery: a) extracted axis using the expansible skeleton model (the sphere represents the cell used for the inertia matrix calculation), b) stack of cross-sectional contours and an example of an image plane locally perpendicular to the axis.

Another model, called expansible skeleton, also uses internal and external forces to control the evolution of the axis [21, 22]. However, this model progressively grows along the vessel and therefore does not include the elasticity force. The initialisation requires a minimum user interaction: selection of a single point on the vessel surface. A starting point within the vessel is then automatically deduced (Fig. 1a). The axis is stretched in the direction of the inertia matrix eigenvector associated with the smallest eigenvalue and is bent by a force which attracts it towards local intensity maxima and which meets the reaction of the flexibility force. As mentioned above, inertia moments also provide an estimate of the vessel size (4), which can be used to initialise the model of the boundaries, although the actual implementation uses the single-point initialisation of the cross-sectional contours, described at the end of the previous sub-section (Fig. 1b).

A model similar to the expansible skeleton represents the axis as a flight-path of particles submitted to elementary attraction and repulsion forces [1]. The particles are attracted by each other and are repulsed by the intensity gradients which are likely to correspond to vessel boundaries. Local flight direction is deduced from the eigenvectors of the inertia matrix.

5. MODELS OF BRANCHING VASCULAR STRUCTURES

One of the limitations of the conventional deformable models is their difficulty to cope with topology changes. Their flexibility is voluntarily bounded so that the extracted boundaries are smooth, without protrusions. Several improvements have been proposed to let the deformable models "penetrate" the branching structures. These generally use a local relaxation of the flexibility constraint in the locations where the distance between the model and the actual boundary is large enough [3, 4, 28, 35]. In addition to the extraction of the boundaries, it is useful to provide a symbolic description of the extracted vascular tree. Theory of graphs provides a convenient model of such structures: nodes represent the bifurcations, while arcs represent the vessel segments. A graph can be constructed using a skeleton obtained by morphological thinning of the previously thresholded image [19, 46]. However, skeleton pruning is a rather difficult operation, since meaningful branches may be mistaken for unwanted spurs. This problem is probably less perceptible when the skeleton is obtained by crest extraction in a “vesselness” map based on the criterion (2) [40]. Detection of significant bifurcations seems to be easier within a careful process of vessel axis tracking. A bifurcation is detected when more than one connected component occurs on the front of the tracking cell [14, 60] or when more than one local depth maximum occurs during a virtual endoscopic exploration [2]. However, spurious depth maxima or connected components may occur. Robustness of the vascular tree description can be significantly improved by fitting the extracted skeleton to a topological model including *a priori* knowledge of the anatomy [5, 55].

5. CONCLUSION AND PERSPECTIVES

Models are very useful in image processing. Their main role is regularisation of ill-posed problems of structure recovery from incomplete and noise-corrupted data. However, simple geometrical models are not sufficient for effective quantitative analysis of 3D vascular images. Models based on knowledge of the anatomy and of the imaging processes are currently being studied. Most of them deal with the vessel lumen and hardly cope with pathological vessel segments, while emphasis should be put on the vessel wall lesions, namely atherosclerotic plaque. The plaque evolves in time, so the models should incorporate this long-range evolution. Moreover, the vessels, especially arteries, are not static. Their axes move following the heart beat, the breathing and the overall body movements. Their walls are extensible and also move according to the heart beat. This motion provides a precious information about the vessel wall health. Hence, future models probably will include the dynamics of the vascular system and multi-modality images will be used to recover both morphological and functional (dynamic) quantitative information.

BIBLIOGRAPHY

[1] Angella F., Lavialle O. and Baylou P., A deformable and expansible tree for structure recovery, Proc. ICIP, pp. 241-245, Chicago, IEEE, 1998.

[2] Bellemare M.E., Haigron P. and Lucas A., Application de la navigation active à la caractérisation automatique de structures anatomiques, Proc. 17e Colloque GRETSI, pp. 1189-1192, Vannes, 1999.

[3] Bulpitt A.J., Segmentation of complex anatomical 3D deformable structures using 3D models, Proc. Med. Image Understanding and Analysis, pp. 189-192, Oxford (UK), 1997.

[4] Bulpitt A.J. and Berry E., An automatic 3D deformable compared with interactive region growing, Proc. Med. Image Understand. and Analysis, pp. 25-28, Leeds (UK), 1998.

[5] Chalopin C., Finet G. and I.E. M., Modeling the 3D coronary tree for labeling purpose, MEDIA, pp. in press, 2001.

[6] Chen H. and Hale J., An algorithm for MR angiography image enhancement, MRM, Vol. 33, pp. 534-540, 1995.

[7] Chen J., Sato Y. and Tamura S., Orientation space filtering for multiple orientation line segmentation, IEEE Trans. Pattern Analysis Machine Intell., Vol. 22, No. 5, 2000.

[8] Chung A.C.S. and Noble J.A., Statistical 3D vessel segmentation using a Rician distribution, Proc. MICCAI, pp. 82-89, Cambridge (UK), Springer Verlag, 1999.

[9] Dokládal P., Lohou C., Perroton L. and Bertrand G., Liver blood vessel extraction by a 3D topological approach, Proc. MICCAI, pp. 98-105, Cambridge (UK), Springer Verlag, 1999.

[10] Du Y.P. and Parker D.L., Digital vessel enhancement filtering of 3D angiograms using long range signal correlation, Proc. 3rd ISMRM, pp. 581, Nice (France), 1995.

[11] Du Y.P., Parker D.L. and Davis W.L., Vessel enhancement filtering in three-dimensional MR angiography, JMRI, Vol. 5, pp. 151-157, 1995.

[12] Feldmar J., Malandain G., Ayache N., Fernández-Vidal S. and Trousset Y., Matching 3D MR angiography data and 2D X-ray angiograms, Proc. CVR Med, pp. 129-138, Grenoble (France), Springer Verlag, 1997.

[13] Fernández-Vidal S. and Malandain G., Squelettes euclidiens d'objets discrets n-dimensionnels, Proc. RFIA, pp. 943-952, Rennes (France), 1996.

[14] Flasque N., Desvignes M., Constans J.-M. and Revenu M., Accurate detection of 3D tubular tree structures, Proc. ICIP, pp. 436-439, Vancouver (Canada), 2000.

[15] Frangi A.F., Niessen W.J., Hoogeveen R.M., van Walsum T. and Viergever M.A., Model-based quantitation of 3D magnetic resonance angiographic images, IEEE Trans. Med. Imaging, Vol. 18, No. 10, pp. 946-956, 1999.

[16] Frangi A.F., Niessen W.J., Hoogeveen R.M., van Walsum T. and Viergever M.A., Quantitation of vessel morphology from 3D MRA, Proc. MICCAI, pp. 358-367, Cambridge (UK), Springer Verlag, 1999.

[17] Frangi A.F., Niessen W.J., Nederkoorn P.J., Elgersma O.E.H. and Viergever M.A., Three-dimensional model-based stenosis quantification of the carotid arteries from contrast-enhanced MR angiography, Proc. Mathematical Methods in Biomedical Image Analysis, pp. 110-118, Hilton Head Island, South Carolina (USA), IEEE Computer Society press, 2000.

[18] Frangi A.F., Niessen W.J., Vincken K.L. and Viergever M.A., Multiscale vessel enhancement filtering, Proc. MICCAI, pp. 130-137, Cambridge, MA (USA), 1998.

[19] Gerig G., Koller T., Szekely G., Brechbühler C. and Kübler O., Segmentation and symbolic description of cerebral vessel structure, based on MR angiography volume data, Proc. CAR, pp. 359-365, Berlin, Springer Verlag, 1993.

[20] Hanka R., Ip H.H.S. and Tang H.Y., Computerised analysis of aortic distensibility on computed tomography, Proc. Current Perspectives in Healthcare Computing, Harrogate, 1997.

[21] Hernández-Hoyos M., Anwander A., Orkisz M., Roux J.-P., Douek P.C. and Magnin I.E., A deformable vessel model with single point initialization for segmentation, quantification and visualization of blood vessels in 3D MRA, Proc. MICCAI, pp. 735-745, Pittsburgh, PA (USA), 2000.
[22] Hernández-Hoyos M., Orkisz M., Roux J.-P. and Douek P., Inertia-based vessel axis extraction and stenosis quantification in 3D MRA images, Proc. Computer Assisted Radiology and Surgery, pp. 189-193, Paris (France), 1999.
[23] Hoogeveen R.M., Bakker C.J.G. and Viergever M.A., Limits to the accuracy of vessel diameter measurement in MRA, JMRI, Vol. 8, No. 6, pp. 1228-1235, 1998.
[24] Hu X., Alperin N., Levin D.N., Tan K.K. and Mengeot M., Visualisation of MR angiography data with segmentation and volume-rendering techniques, JMRI, Vol. 1, pp. 539-546, 1991.
[25] Krissian K., Malandain G. and Ayache N., Model based multiscale detection and reconstruction of 3D vessels, Report # 3442, INRIA, Sophia Antipolis (France), 1998.
[26] Krissian K., Malandain G., Ayache N., Vaillant R. and Trouuset Y., Model based multiscale reconstruction of 3D vessels, Proc. CVPR, pp. 722-727, Santa Barbara, CA, IEEE, 1998.
[27] Kutka R. and Stier S., Extraction of line properties based on direction fields, IEEE Trans. Med. Imaging, Vol. 15, No. 1, pp. 51-58, 1996.
[28] Ladak H.M., Milner J.S. and Steinman D.A., Rapid three-dimensional segmentation of the carotid bifurcation from serial MR images, J. Biomech. Engineering, Vol. 112, pp. 96-99, 2000.
[29] Li L., Mao F., Qian W. and Clarke L.P., Wavelet transform for directional feature extraction in medical imaging, Proc. ICIP, pp. 500-503, Sta Barbara, CA (USA), 1997.
[30] Loock T., Westin C.F., Haglund L., Wigström L., Sjöquist L. and Knutsson H., Multidimensional adoptive filtering of 3D MRA data, Proc. 3rd ISMRM, pp. 716, Nice (France), 1995.
[31] Lorenz C., Carlsen I.-C., Buzug T.M., Fassnacht C. and Weese J., Multiscale line segmentation with automatic estimation of width, contrast and tangential direction in 2D and 3D medical images, Proc. CVR Med, pp. 233-242, Grenoble (France), Springer Verlag, 1997.
[32] Lorigo L.M., Faugeras O., Grimson W.E.L., Keriven R., Kikinis R. and Westin C.-F., Co-dimension 2 geodesic active contours for MRA segmentation, Proc. Int. Conf. Informations Processing Med. Imaging, Visegrad (H), Springer Verlag, 1999.
[33] Masutani Y., Schiemann T. and Höhne K.-H., Vascular shape segmentation and structure extraction using a shape-based region growing model, Proc. MICCAI, pp. 1242-1249, Cambridge, MA (USA), 1998.
[34] McInerney T. and Terzopoulos D., Deformable models in medical image analysis : a survey, Med. Image Analysis, Vol. 1, No. 2, pp. 91-108, 1996.
[35] McInerney T. and Terzopoulos D., Medical image segmentation using topologically adaptable surfaces, Proc. CVR Med, pp. 23-32, Grenoble (France), Springer Verlag, 1997.
[36] Orkisz M., Bresson C., Magnin I.E., Champin O. and Douek P.C., Improved vessel visualization in MR angiography by non-linear anisotropic filtering, Magnetic Resonance in Medicine, Vol. 37, pp. 914-919, 1997.
[37] Orkisz M., Hernández-Hoyos M., Douek P. and Magnin I., Advances of blood vessel morphology analysis in 3D magnetic resonance images, Machine Graphics & Vision, Vol. 9, No. 1/2, pp. 463-471, 2000.
[38] Pasquignon D., Calcul du squelette par équation aux dérivées partielles, Proc. RFIA, pp. 934-942, Rennes (France), 1996.
[39] Prinet J., Monga O. and Ma D.S., Extraction of vascular network in 3D images, Proc. ICIP, pp. 307-310, Lausanne (Switzerland), 1996.
[40] Prinet V., Monga O. and Rocchisani J.-M., Vessel representation in 2D and 3D angiograms, Proc. CAR, pp. 240-245, Berlin, Elsevier, 1997.
[41] Rueckert D. and Burger P., A multiscale approach to contour fitting for MR images, Proc. Med. Imaging Image Processing, Newport Beach, SPIE, 1996.
[42] Rueckert D. and Burger P., Shape-based tracking and analysis of the aorta in cardiac MR images using geometrically deformable templates, Proc. CAR, pp. 26-29, Paris (France), 1996.
[43] Rueckert D., Burger P., Forbat S.M., Mohiaddin R.D. and Yang G.Z., Automatic tracking of the aorta in cardiovascular MR images using deformable models, IEEE Trans. Med. Imaging, Vol. 16, No. 5, pp. 581-590, 1997.
[44] Sato Y., Nakajima S., Atsumi H., Koller T., Gerig G., Yoshida, S. and Kikinis, R., 3D multiscale line filter for segmentation and visualization of curvilinear structures in medical images, Proc. CVR Med, pp. 213-222, Grenoble (France), Springer Verlag, 1997.

[45] Sato Y., Nakajima S., Shiraga N., Atsumi H., Yoshida, S., Koller T., Gerig G. and Kikinis, R., 3D multi-scale line filter for segmentation and visualization of curvilinear structures in medical images, Med. Image Analysis, Vol. 2, No. 2, pp. 143-168, 1998.
[46] Sauret V., Goatman K.A., Fleming J.S. and Bailey A.G., 3D topology and morphology of branching networks using computed tomography (CT) - application to the airway tree, Proc. Medical Image Understanding and Analysis, Oxford (UK), 1999.
[47] Shafer S.A., Shadows and Silhouettes in Computer Vision, Kluwer Academic Publishers, Boston, 1985.
[48] Staib L.H. and Duncan J.S., Boundary finding with parametrically deformable models, IEEE Pattern Analysis Machine Intell., Vol. 14, No. 11, pp. 1061-1075, 1992.
[49] Stern C., Wildermuth S., Weissmann J., Stucki P., Hilfiker, P. and Debatin, J.F., Interactive definition of endoluminal aortic stent size and morphology based on virtual angioscopic rendering of 3D MRA, Proc. CARS, pp. 176-180, Paris (France), 1999.
[50] Swift R.D., Ramaswamy K. and Higgins W.E., Adaptive axes-generation algorithm for 3D tubular structures, Proc. ICIP, pp. 136-139, Sta Barbara, CA (USA), 1997.
[51] Vandermeulen D., Delaere D., Suetens P., Bosmans M. and Marchal G., Local filtering and global optimization methods for 3D magnetic resonance angiography (MRA) image enhancement, Proc. Visualization in Biomedical Computing, pp. 274-288, Chapel Hill, NC (USA), SPIE, 1992.
[52] Verdonck B., Bloch J., Maître H., Vandermeulen D., Suetens P. and Marchal G., Accurate segmentation of blood vessels from 3D medical images, Proc. ICIP, pp. 311-314, Lausanne (Switzerland), 1996.
[53] Verdonck B., Bloch J., Maître H., Vandermeulen D., Suetens P. and Marchal G., Blood vessel segmentation and visualization in 3D MRA and spiral CT angiography, Proc. CAR, pp. 177-182, Berlin, Springer Verlag, 1995.
[54] Wilson D.L. and Noble J.A., Segmentation of cerebral vessels and aneurysms from MR angiography data, Proc. 15th Int.Conf. Information Processing in Med. Imaging, pp. 423-428, Springer Verlag, 1997.
[55] Wilson L.S., Brown S.F., Young J.A., Li R. and Brandt L., Three-dimensional computer models of abdominal aortic aneurysms by knowledge-based segmentation, Proc. CARS, pp. 213-217, Paris (France), 1999.
[56] Wink O., Niessen S.J. and Viergever M.A., Minimum cost path determination using a simple heuristic function, Proc. ICPR, Vol. 3, pp. 1010-1013, Barcelona, 2000.
[57] Wink O., Niessen W.J. and Viergever M.A., Fast quantification of abdominal aortic aneurysums from CTA volumes, Proc. MICCAI, pp. 138-145, Cambridge, MA (USA), 1998.
[58] Wink O., Niessen W.J. and Viergever M.A., Fast delineation and visualization of vessel in 3D angiography images, IEEE Trans. Med. Imaging, Vol. 19, No. 4, pp. 337-346, 2000.
[59] Wink O., Niessen W.J., Wever J.J. and Broeders I.A.J.M., Semi-automated quantification and segmentation of abdominal aorta aneurysins from CTA volumes, Proc. CARS, pp. 208-212, Paris (France), 1999.
[60] Zahlten C., Jürgens H. and Peitgen H.-O., Reconstuction of branching blood vessel from CT data, Proc. Visualization in Scient. Comput., pp. 41-52, 1994.